World Journal of Gastroenterology

Submit a Manuscript: http://www.f6publishing.com

World J Gastroenterol 2017 November 21; 23(43): 7765-7775

DOI: 10.3748/wjg.v23.i43.7765

ISSN 1007-9327 (print) ISSN 2219-2840 (online)

ORIGINAL ARTICLE

Clinical Trials Study

Application of superb microvascular imaging in focal liver lesions

Meng-Na He, Ke Lv, Yu-Xin Jiang, Tian-An Jiang

Meng-Na He, Ke Lv, Yu-Xin Jiang, Department of Ultrasound, Peking Union Medical College Hospital, Peking Union Medical College, Chinese Academy of Medical Sciences, Beijing 100730, China

Tian-An Jiang, Department of Ultrasound, The First Affiliated Hospital, College of Medicine, Zhejiang University, Hangzhou 310000, Zhejiang Province, China

ORCID number: Meng-Na He (0000-0002-8178-3531); Ke Lv (0000-0001-8779-9860); Yu-Xin Jiang (0000-0003-3430-4080); Tian-An Jiang (0000-0002-7672-8394).

Author contributions: He MN, Lv K, and Jiang YX designed the research; He MN and Lv K performed the research; Jiang TA contributed new reagents or analytic tools and analyzed the data; He MN wrote the paper.

Institutional review board statement: The study was reviewed and approved by the ethical committee of Peking Union Medical College Hospital.

Informed consent statement: Informed consent was provided by each patient before examination.

Conflict-of-interest statement: This article has no conflict of interests to disclose.

Data sharing statement: No additional data are available.

Manuscript source: Unsolicited manuscript

Correspondence to: Yu-Xin Jiang, MD, Department of Ultrasound, Peking Union Medical College Hospital, Peking Union Medical College, Chinese Academy of Medical Sciences, Beijing 100730, China. jiangyuxinxh@163.com
Telephone: +86-10-69155494
Fax: +86-10-69155494

Received: August 13, 2017
Peer-review started: August 15, 2017
First decision: August 30, 2017
Revised: September 14, 2017
Accepted: September 19, 2017
Article in press: September 19, 2017
Published online: November 21, 2017

Abstract

AIM

To explore the ability of superb microvascular imaging (SMI) in differential diagnosis of focal liver lesions (FLLs) and to compare SMI morphology findings to those of color Doppler ultrasound and enhanced imaging.

METHODS

Twenty-four patients with 31 FLLs were included in our study, with diagnoses of hemangioma (HE) (n = 17), hepatocellular carcinoma (HCC) (n = 5), metastatic lesions (n = 5), primary hepatic lymphoma (n = 1), focal nodular hyperplasia (FNH) (n = 2), and adenoma (n = 1). Nine lesions were pathologically diagnosed, and 22 lesions were radiologically confirmed, all of which were evaluated by at least two types of enhanced imaging techniques. All patients had undergone SMI. Patients were divided into subgroups based on pathological and radiological diagnoses to analyze SMI manifestations. We also compared the SMI manifestations of the most common malignant FLLs (HCCs and metastatic lesions) with those of the most common benign FLLs (HEs).

RESULTS

HEs were classified into three SMI subgroups: diffuse dot-like type (n = 6), strip rim type (n = 8), and

nodular rim type (n = 3). The sizes of the three types of HEs were significantly different (P = 0.00, < 0.05). HCCs were classified into two subgroups: diffuse honeycomb type (n = 2) and non-specific type (n = 3). Four of the metastatic lesions were the strip rim type, and the other metastatic lesion was the thick rim type, which is the same as that of lymphoma. FNH was described as a spoke-wheel type, and adenoma as a diffuse honeycomb type. The SMI types of HCCs and metastatic lesions were significantly different from those of HEs (P = 0.048, < 0.05).

CONCLUSION

SMI technology enables microvascular evaluation of FLLs without using any contrast agent. For HEs, lesion size may affect SMI performance. SMI is able to provide useful information for differential diagnosis of HCCs and metastatic lesions from HEs.

Key words: Primary hepatic lymphoma; Hemangioma; Color doppler ultrasound; Focal liver lesions; Superb microvascular imaging

Core tip: We utilized a novel ultrasound technique, superb microvascular imaging (SMI), to assess the microvascular morphology of focal liver lesions to provide additional diagnostic information. The focal liver lesions consisted of hemangiomas, hepatocellular carcinomas, metastatic lesions, primary hepatic lymphoma, focal nodular hyperplasia, and adenoma. We also compared SMI manifestations to color Doppler ultrasound and enhanced imaging features.

He MN, Lv K, Jiang YX, Jiang TA. Application of superb microvascular imaging in focal liver lesions. *World J Gastroenterol* 2017; 23(43): 7765-7775 Available from: URL: http://www.wjgnet.com/1007-9327/full/v23/i43/7765.htm DOI: http://dx.doi.org/10.3748/wjg.v23.i43.7765

INTRODUCTION

The detection rate of focal liver lesions (FLLs) is clearly increasing because of the widespread application of imaging techniques, especially ultrasound examinations. Kaltenbach *et al*[1] investigated 45319 hospitalized patients and found that the prevalence of benign FLLs was 15.1%. Hepatocellular carcinoma (HCC) is the second most common cause of mortality from cancer[2,3]. The current diagnostic challenge not only involves effectively distinguishing between malignant and benign FLLs[4,5] but also precisely identifying the characteristics of all types of FLLs since they require different clinical treatments and have different outcomes. For example, treatments for hemangioma (HE) and adenoma and those for HCC and lymphoma differ significantly.

To address this challenge, it is essential to establish a diagnostic method that is inexpensive, easy to operate, and has high diagnostic accuracy. Contrast-enhanced ultrasound (CEUS) has been gradually recognized as a comparable imaging technique to contrast-enhanced computed tomography (CECT) and contrast-enhanced magnetic resonance imaging (CEMRI) in the diagnosis of FLLs[6,7]. The common advantage of the above three techniques is visualization of the microvascular structure, which is one of the most important elements of the tumor microenvironment[8], plays an important role in the development and progression of lesions, and is essential for their differential diagnosis. However, these techniques also have drawbacks. Some patients may be ineligible for these examinations because of contraindications to contrast agents, such as the risk of triggering or worsening renal failure with the iodinated contrast agents used for computed tomography (CT) and gadolinium diethylene-trianmine pentaacetic acid (Gd-DTPA) used for magnetic resonance imaging (MRI)[9], as well as the risk of hypersensitivity reactions caused by the agents used in CEUS, CECT, and CEMRI[10]. Additionally, these techniques are expensive and time-consuming, limiting their widespread use.

Superb microvascular imaging (SMI) is a novel Doppler technique developed by Toshiba Medical System (Tokyo, Japan)[11], which was designed to simulate CEUS by using advanced clutter elimination to obtain only vascular flow signals without using any contrast agents[12]. Similar to color Doppler and power Doppler imaging, SMI can provide a real-time examination of vascularity in FLLs, but it has the additional advantages of detecting slower blood flow and revealing micro-vessels. Studies on SMI technology in superficial tissues, such as thyroid and breast tumors, have been reported, with some useful information obtained for differential diagnoses[11,13]. Machado *et al*[13] evaluated the capability of SMI to show microvascular flow in normal thyroid tissue and in thyroid nodules compared with that of CDFI and found that SMI was able to better depict vessel branching. Zhan *et al*[14] compared the abilities of CDFI and SMI to reveal penetrating vessels (PVs) in breast cancer and discovered that more PVs were evident by SMI than by CDFI. By contrast, very few studies have been conducted on SMI for FLLs[15]. The purpose of this study was to investigate the SMI features of FLLs and to analyze the ability of SMI to provide additional information for the differential diagnosis of FLLs.

MATERIALS AND METHODS

Patients and FLLs

This study was performed from November 2016 to March 2017 at Peking Union Medical College Hospital. The study was approved by the ethical committee of the hospital, and informed consent was provided by

Table 1 Characteristics of focal liver lesions and corresponding patients

No.	Clinical diagnosis	Pathological diagnosis	SMI type (Ⅰ-Ⅶ)	Size (cm)	Age (yr)	Sex	Other
1	HE	-	Ⅰ	1.7	79	M	
2	HE	-	Ⅰ	1.1	58	F	
3	HE	-	Ⅰ	2.6	54	M	
4	HE	-	Ⅰ	2.5	52	F	
5	HE	-	Ⅰ	1.8	24	F	Same person
6	HE	-	Ⅰ	2.7	24	F	
7	HE	-	Ⅱ	2.3	63	M	
8	HE	-	Ⅱ	3.9	61	M	Same person
9	HE	-	Ⅱ	4.8	61	M	
10	HE	-	Ⅱ	3.7	61	F	
11	HE	-	Ⅱ	2.8	48	M	Same person
12	HE	-	Ⅱ	3.1	48	M	
13	HE	-	Ⅱ	3.1	41	M	
14	HE	-	Ⅱ	5.7	33	F	
15	HE	-	Ⅲ	6.3	63	F	
16	-	HE	Ⅲ	8.4	51	F	
17	-	HE	Ⅲ	8.5	47	F	
18	B-M	-	Ⅱ	1.4	39	F	Same person
19	B-M	-	Ⅱ	2.3	39	F	
20	B-M	-	Ⅱ	2.6	39	F	
21	B-M	-	Ⅱ	3.3	39	F	
22	P-M	-	Ⅵ	3.9	64	M	
23	-	HCC	Ⅳ	7.4	68	M	
24	-	HCC	Ⅳ	6.1	57	M	
25	-	HCC	Ⅴ	2.5	60	M	
26	-	HCC	Ⅴ	2.9	48	M	Same person
27	-	HCC	Ⅴ	4.7	48	M	
28	-	HA	Ⅳ	5.3	41	M	
29	-	LYM	Ⅵ	5.8	71	M	
30	FNH	-	Ⅶ	4.1	62	F	
31	FNH	-	Ⅶ	4.3	39	F	

Type Ⅰ: Diffuse dot-like type; Type Ⅱ: Strip rim type; Type Ⅲ: Nodular rim type; Type Ⅳ: Diffuse honeycomb type; Type Ⅴ: Non-specific type; Type Ⅵ: Thick rim type; Type Ⅶ: Spoke-wheel type; FLL: Focal liver lesion; HE: Hemangioma; B-M: Metastatic lesion from breast; P-M: Metastatic lesion from pancreas; M: Metastatic lesion; HCC: Hepatocellular carcinoma; FNH: Focal nodular hyperplasia; HA: Hepatic adenoma; PHL: Primary hepatic lymphoma.

each patient before examination. Twenty-four patients (mean age, 53.5 ± 12.9 years, range 24-79 years; 13 men and 11 women) with 31 FLLs were included in our study. All FLLs had been detected by at least two modalities of CEUS/CT/MRI. Of all FLLs, nine were pathologically diagnosed, including two HEs in two patients, five HCCs in four patients, one hepatic adenoma, and one primary hepatic lymphoma, and 22 were radiologically confirmed, including 15 HEs in 12 patients (a single lesion in nine patients and two lesions in three patients), which were diagnosed by CECT and/or CEMRI and showed typical manifestations of nodular or strip type, with peripheral to centripetal enhancement and persistent enhancement in the portal venous phase and the delayed phase. Five metastatic masses (one patient had a single lesion and another patient had four lesions) were diagnosed by the primary tumor history and CECT/CEUS, which showed malignant characteristics with arterial enhancement that disappeared quickly in the portal venous phase. Two focal nodular hyperplasia (FNH) lesions were diagnosed by CECT based on persistent enhancement from the arterial phase to the portal venous/delayed phase, clearly defined outlines, and a central scar. Table 1 summarizes the clinical, SMI, and pathologic features of the 31 FLLs.

SMI examination and imaging analysis

Patients were placed in the supine or left lateral position after 6 h of fasting. All US examinations, including B-mode US, CDFI, and SMI, were performed with a curved transducer (6C1Aplio 500; Toshiba Medical Systems Corporation, Tochigi, Japan). B-mode US was performed first to thoroughly scan the liver for FLLs. Once detected, the general features of FLLs were observed and their sizes (maximal diameter) were measured. Subsequently, conventional CDFI and SMI were performed to observe the vascular structures of the FLLs. For the CDFI examination, the scale was set as low as possible until the appropriate level was reached without any pseudo color flow, such as color flow spillover (the lowest scale was 4 cm/s), and the flow gain was adjusted until noise emerged. For the SMI examination, the parameter settings were as follows: color velocity scale of no more than 2.0 cm/s, frame rate > 30 fps, color frequency 5-7 MHz, and the gain setting adjusted to show optimal imaging. All US examinations were performed by a single operator, and

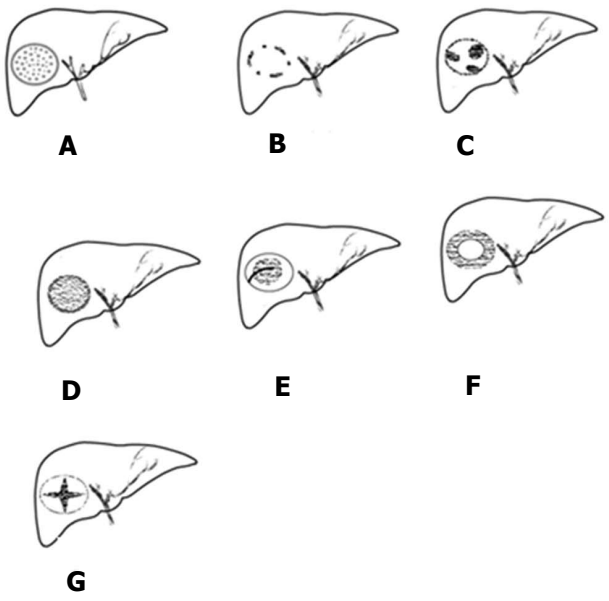

Figure 1 A simplified diagram of the seven superb microvascular imaging types. A: Type Ⅰ, diffuse dot-like type; B: Type Ⅱ, strip rim type; C: Type Ⅲ, nodular rim type; D: Type Ⅳ, diffuse honeycomb type; E: Type Ⅴ, non-specific type; F: Type Ⅵ, thick rim type; G: Type Ⅶ, spoke-wheel type.

Table 2 Size, average age, and sex distribution of the three types of hemangiomas

Type	Size	Yr	Sex
Ⅰ	2.07 ± 0.63	48.5 ± 21.3	2\4
Ⅱ	3.68 ± 1.12	52.0 ± 11.2	6\2
Ⅲ	7.73 ± 1.24	53.7 ± 8.3	0\3
P value	0	0.89	0.06

Type Ⅰ: Diffuse dot-like type; Type Ⅱ: Strip rim type; Type Ⅲ: Nodular rim type.

the imaging data were analyzed by two experienced radiologists. Both the operator and readers had > 10 years of experience in liver ultrasound. The readers classified the SMI characteristics of the FLLs into seven types (Figure 1): Ⅰ, diffuse dot-like type; Ⅱ, strip rim type; Ⅲ, nodular rim type; Ⅳ, diffuse honeycomb type; Ⅴ, non-specific type; Ⅵ, thick rim type with lymphoma; and Ⅶ, spoke-wheel type[15]. If a disagreement occurred, the decision was determined by consensus after consultation with a third experienced doctor. We divided the 31 FLLs into a ⩽ 3.0 cm group and a > 3.0 cm group[16], and then compared vascular visibility between CDFI and SMI. We also compared the SMI types of the most common malignant FLLs (HCCs and metastatic lesions) and those of the most common benign FLLs (HEs).

Statistical analysis

Differences in SMI types between the most common malignant FLLs (HCCs and metastatic lesions) and the most common benign FLLs (HEs) were evaluated by Fisher's exact test. The χ^2 test was used to compare the sex distribution of HEs between different SMI types. Differences in size and age were evaluated by a one-way ANOVA test. $P < 0.05$ was considered statistically significant. SPSS 16.0 was used for all data analyses.

RESULTS

All 31 FLLs underwent successful US examinations, including B-mode US, CDFI, and SMI, and satisfactory images were obtained. Of the 17 HEs, the SMI features could be divided into three types: diffuse dot-like type (Type Ⅰ; *n* = 6; Figure 2), strip rim type (Type Ⅱ; *n* = 8; Figure 3), and nodular rim type (Type Ⅲ; *n* = 3; Figure 4). The sizes of the three types of HEs were significantly different (*P* = 0.00, < 0.05), but the average age and sex distributions of the patients showed no significant differences (Table 2).

The SMI features of the 14 remaining FLLs were as follows: two of the HCCs were described as the diffuse honeycomb type (Type Ⅳ, Figure 5) and three were defined as the non-specific type (Type Ⅴ, Figure 6). Four of the metastatic lesions were from breast cancer in one patient and were classified as the strip rim type (Type Ⅱ), and one was from pancreatic cancer and was classified as the thick rim type (Type Ⅵ, Figure 7), with the lesion reflecting primary hepatic lymphoma. Two FNH lesions were described as the spoke-wheel type (Type Ⅶ, Figure 8), and the adenoma was described as the diffuse honeycomb type (Type Ⅴ). The distributions of SMI types between the most common malignant FLLs (HCCs and metastatic lesions) and the most common benign FLLs (HEs) were significantly different (*P* = 0.048, < 0.05) (Table 3), and these morphological findings of SMI types in different FLLs were consistent with the findings from contrast-enhanced ultrasound/CT/MRI. The characteristics of all FLLs and the corresponding patients are summarized in Table 1.

Among the 31 FLLs, 13 were small FLLs with a maximum diameter of less than 3.0 cm and 17 were larger than 3.0 cm. SMI could detect the vascular structures of all 31 lesions, while CDFI failed to detect the vascular structures of nine (69.2%) lesions in the < 3.0 cm group and two (11.8%) lesions in the > 3.0 cm group.

DISCUSSION

Angiogenesis, an important part of the tumor microenvironment[17], plays a key role in the development of FLLs. The morphology of blood vessels in lesions is also important for differential diagnoses. CDFI had been widely used to depict tumor vessels, but it is limited in identifying low-speed flow signals because of the wall filter, which suppresses clutter and motion artifacts and results in the loss of low-speed flow signals. SMI, a novel technique, can overcome this limitation and can effectively distinguish low-speed flow signals from

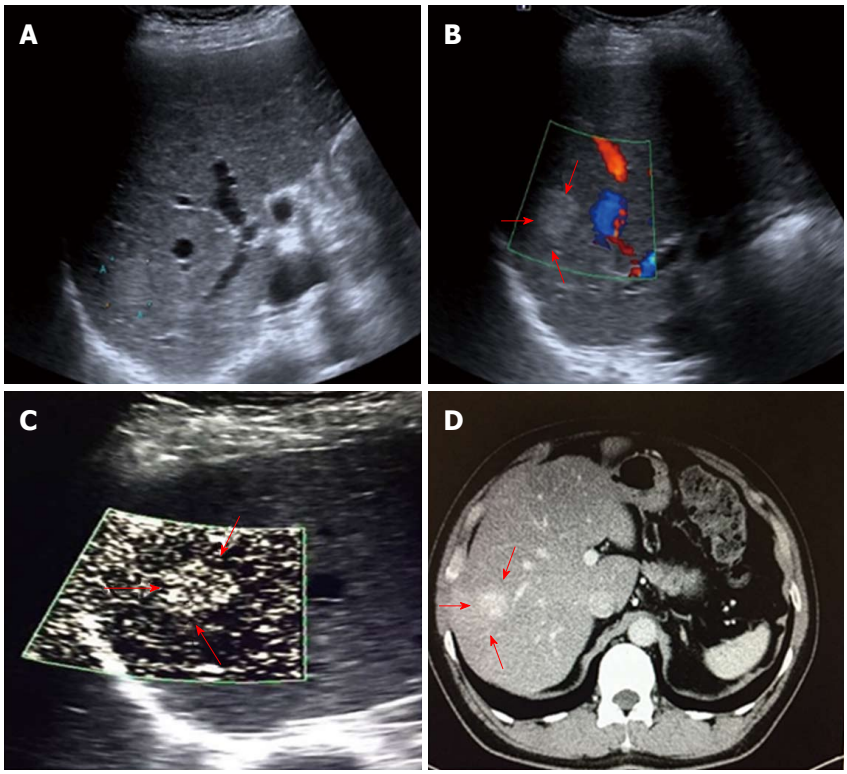

Figure 2 Diffuse dot-like type (type Ⅰ) in a 52-year-old male diagnosed with hemangioma. A: A high-echo lesion with a clear margin was evident in the right liver lobe; B: CDFI showed no blood flow signals for this lesion; C: SMI showed a diffuse dot-like microvascular structure; D: Contrast-enhanced CT showed diffuse enhancement of the lesion in the arterial phase. SMI: Superb microvascular imaging.

Table 3 Distributions of the superb microvascular imaging types in focal liver lesions *n* (%)

Group	Ⅰ	Ⅱ	Ⅲ	Ⅳ	Ⅴ	Ⅵ	Ⅶ
HE (17)	6 (35.2)	8 (47.1)	3 (17.6)	0 (0)	0 (0)	0 (0)	0 (0)
M (5)	0 (0)	4 (80)	0 (0)	0 (0)	0 (0)	1 (20)	0 (0)
HCC (5)	0 (0)	0 (0)	0 (0)	2 (40)	3 (60)	0 (0)	0(0)
FNH (2)	0 (0)	0 (0)	0 (0)	0 (0)	0 (0)	0 (0)	2 (100)
HA (1)	0 (0)	0 (0)	0 (0)	1 (100)	0 (0)	0 (0)	0 (0)
PHL (1)	0 (0)	0 (0)	0 (0)	0 (0)	0 (0)	1 (100)	0 (0)

The distributions of the superb microvascular imaging types between the most common malignant focal liver lesions (hepatocellular carcinoma and metastatic lesions) and the most common benign focal liver lesions (hemangiomas) were significantly different (P = 0.048, < 0.05). Type Ⅰ: Diffuse dot-like type; Type Ⅱ: Strip rim type; Type Ⅲ: Nodular rim type; Type Ⅳ: Diffuse honeycomb type; Type Ⅴ: Non-specific type; Type Ⅵ: Thick rim type; Type Ⅶ: Spoke-wheel type; HE: Hemangioma; M: Metastatic lesion; HCC: Hepatocellular carcinoma; FNH: Focal nodular hyperplasia; HA: Hepatic adenoma; PHL: Primary hepatic lymphoma.

artifacts without the use of any contrast agent. In the current study, we compared the abilities of CDFI and SMI to detect the vascular structures of all 31 FLLs, and the results showed that SMI could detect flow information in all lesions, but CDFI failed to detect the vascular structures of nine (69.2%) lesions in the < 3.0 cm group and two (11.8%) lesions in the > 3.0 cm group, suggesting that SMI has obvious advantages in detecting the blood vessels of FLLs. Therefore, SMI overcomes the limitation of CDFI, especially for the description of micro-vessels in small lesions.

Studies on the application of SMI for FLLs are limited, and only two investigations have been reported: one was reported by Wu *et al*[18], in which SMI clearly demonstrated the typical spoke-wheel vascular type of FNH in the liver without the use of any contrast agent, and the other was reported by Lee *et al*[15], who used SMI for 29 FLLs, including HE, HCC, and FNH, and concluded that the SMI types were significantly different between FLLs. In the present study, we analyzed the SMI features of 31 FLLs, including HEs, HCC, metastatic lesions, FNH, hepatic adenoma, and primary hepatic lymphoma. We used seven SMI types to depict the vessel distributions and morphologies of the 31 FLLs. We found that the SMI type distribution between the most common malignant FLLs (HCCs and metastatic lesions) and the most common benign FLLs (HEs) differed significantly, which could provide meaningful differential diagnostic information. Meanwhile, we also found that various

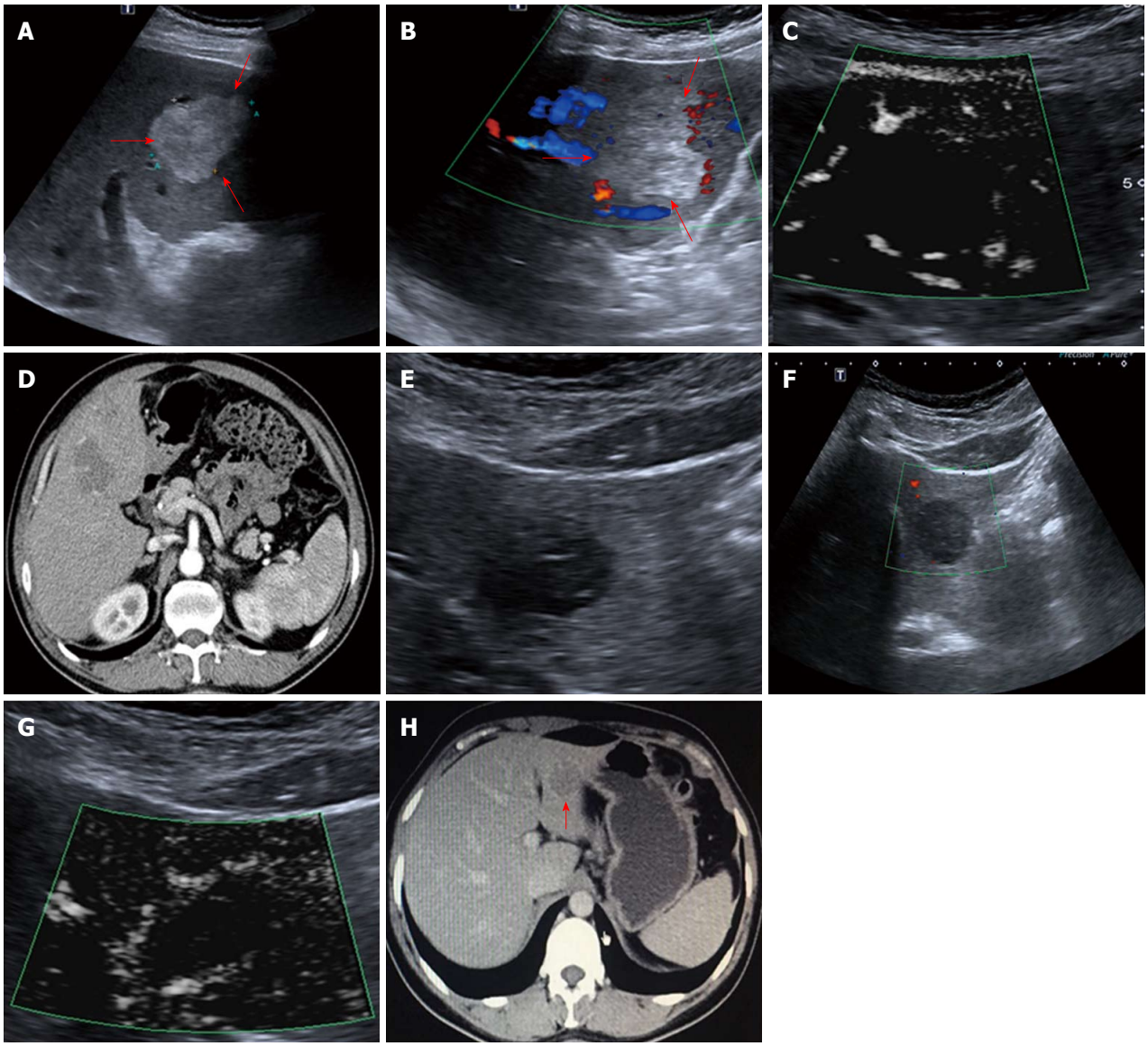

Figure 3 Strip rim type (type Ⅱ). A-D: A 61-year-old male diagnosed with hemangioma. A: A high-echo lesion with a clear margin was evident in the left liver lobe; B: CDFI showed an interrupted strip blood flow signal around the edge of this lesion; C: SMI showed a relatively continuous strip rim-distributed microvascular structure; D: Contrast-enhanced CT showed strip rim enhancement of the lesion in the arterial phase. E-H: A 63-year-old male diagnosed with hemangioma. E: A low-echo lesion with a clear margin was evident in the left liver lobe; F: CDFI showed no blood flow signal for this lesion; G: SMI showed a continuous strip rim microvascular structure; H: Contrast-enhanced CT showed strip rim enhancement of the lesion in the arterial phase. SMI: Superb microvascular imaging.

FLLs shared the same SMI type. For example, the metastatic lesions from breast cancer and HEs shared the strip rim type (Type Ⅱ), and the other metastatic lesion from pancreatic cancer and primary hepatic lymphoma both showed the thick rim type (Type Ⅵ). Hepatic adenoma and some HCCs had the same diffuse honeycomb type (Type Ⅳ). Therefore, when an FLL is suspected to be a certain SMI type, other clinical information, such as a medical history, is still needed to determine an accurate diagnosis.

For HEs, the average maximum diameters of type Ⅰ, type Ⅱ, and type Ⅲ lesions were 2.07 ± 0.63 cm, 3.68 ± 1.12 cm, and 7.73 ± 1.24 cm, respectively, and the lesion sizes of the three different SMI types were significantly different. The histology of the HEs can explain the SMI manifestations. First, the original etiology of HEs was not clear, but congenital vessel malformation caused by hyperplastic endothelial cells may be the cause[19]. Consequently, the microscopic features of HEs appeared like a blood pool constituted by cavernous vascular spaces, which were lined by a single layer of flat endothelial cells of different sizes. The vascular cavities varied in size and corresponded to the size of HE lesions. Some HEs may contain a thrombus that will gradually turn into a fibrous scar or nodules, especially in large lesions[20]. Therefore, for larger HEs, the internal blood flow may be slower or even completely replaced by the thrombus, so an enhanced examination can reveal peripheral nodules or ring-enhanced patterns. SMI also reveals these features, especially in type Ⅱ and type Ⅲ. For small HEs, both enhanced techniques and SMI could show

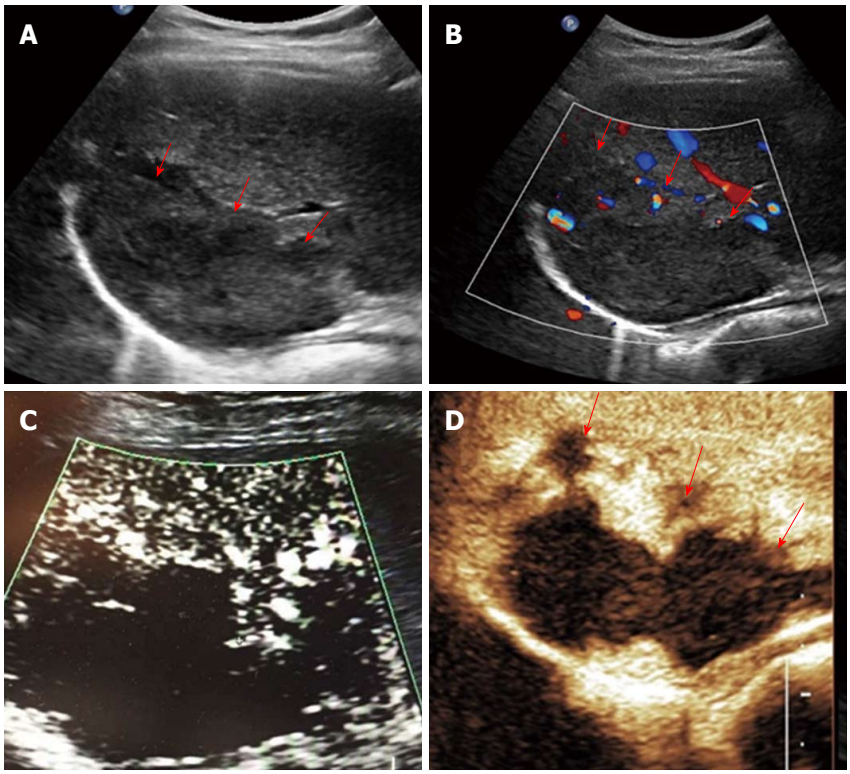

Figure 4 Nodular rim type (type Ⅲ) in a 51-year-old female diagnosed with hemangioma. A: A mixed-echo lesion with a relatively clear margin was evident in the right liver lobe; B: CDFI showed a sporadic short strip blood flow signal around the edge of this lesion; C: SMI showed a nodular rim-distributed microvascular structure; D: Contrast-enhanced ultrasound showed nodular rim enhancement of the lesion in the arterial phase. SMI: Superb microvascular imaging.

slow internal vascular signals, as in type Ⅰ. According to the previous statements, type Ⅰ and type Ⅲ had distinctive features enabling the discrimination of HEs from other FLLs.

Regarding the other types of FLLs, the previous SMI study on FLLs by Lee *et al*[15] showed that the SMI manifestations of HCCs revealed non-specific vascular types, while in the present study, we used two SMI types to summarize HCCs, including type Ⅳ, the diffuse honeycomb type, and type Ⅴ, the non-specific type. The general pathology of the former type showed that the inter-tumor blood vessels were distributed in a grid pattern resembling honeycombs. The SMI feature of the latter type was a strip-like trunk with tiny branches, but we do not have enough evidence from other enhanced techniques or pathology to support it. Therefore, we classified it as the non-specific type. In this research, including two cases of FNH with both CDFI and SMI showing the typical spoke-wheel type without a basic echo of the liver parenchyma, SMI seemed to show the vascular structure more clearly, which is consistent with the previous studies[15,18].

For metastatic lesions, it is always assumed that their imaging results are particularly confusing because metastatic lesions can simulate various other types of FLLs, as in the present study. The SMI types of metastatic lesions were similar to those of HEs and lymphoma. Therefore, in the diagnosis of metastatic lesions, a clinical history including the primary tumor is critical in addition to imaging studies.

Research on the ultrasound features of hepatic adenomas is relatively rare because of the low morbidity compared to other FLLs. Dong *et al*[21] conducted a retrospective study to analyze differences in ultrasound and CEUS features between hepatic adenoma and HCC, and the results showed that most cases of hepatic adenomas manifested as homogenous, rapid, and complete enhancement in the arterial phase, which is similar to HCC. In this study, our case of hepatic adenoma showed the same SMI type (type Ⅳ, diffuse honeycomb type) as some HCCs. This patient was diagnosed with a benign lesion or a relatively mild malignant mass before surgery because of the very clear margin and the slow wash-out pattern on CECT. SMI for this case did not show unique characteristic performance and was limited to the diagnosis of hepatic adenoma, requiring supplementation with an enhanced imaging examination.

Primary hepatic lymphoma (PHL) is also a rare disease, accounting for only 0.016% of all cases of non-Hodgkin's lymphoma (NHL)[22]. The treatment for PHL includes surgery, chemotherapy, and radiotherapy, which is significantly different from that for HCC or other malignant FLLs. Therefore, an accurate diagnosis before surgery is essential. Research by Lu *et al*[23] showed that one CECT manifestation of some PHLs was rim-like enhancement, which was similar to the features revealed by CEUS and SMI. Therefore, SMI

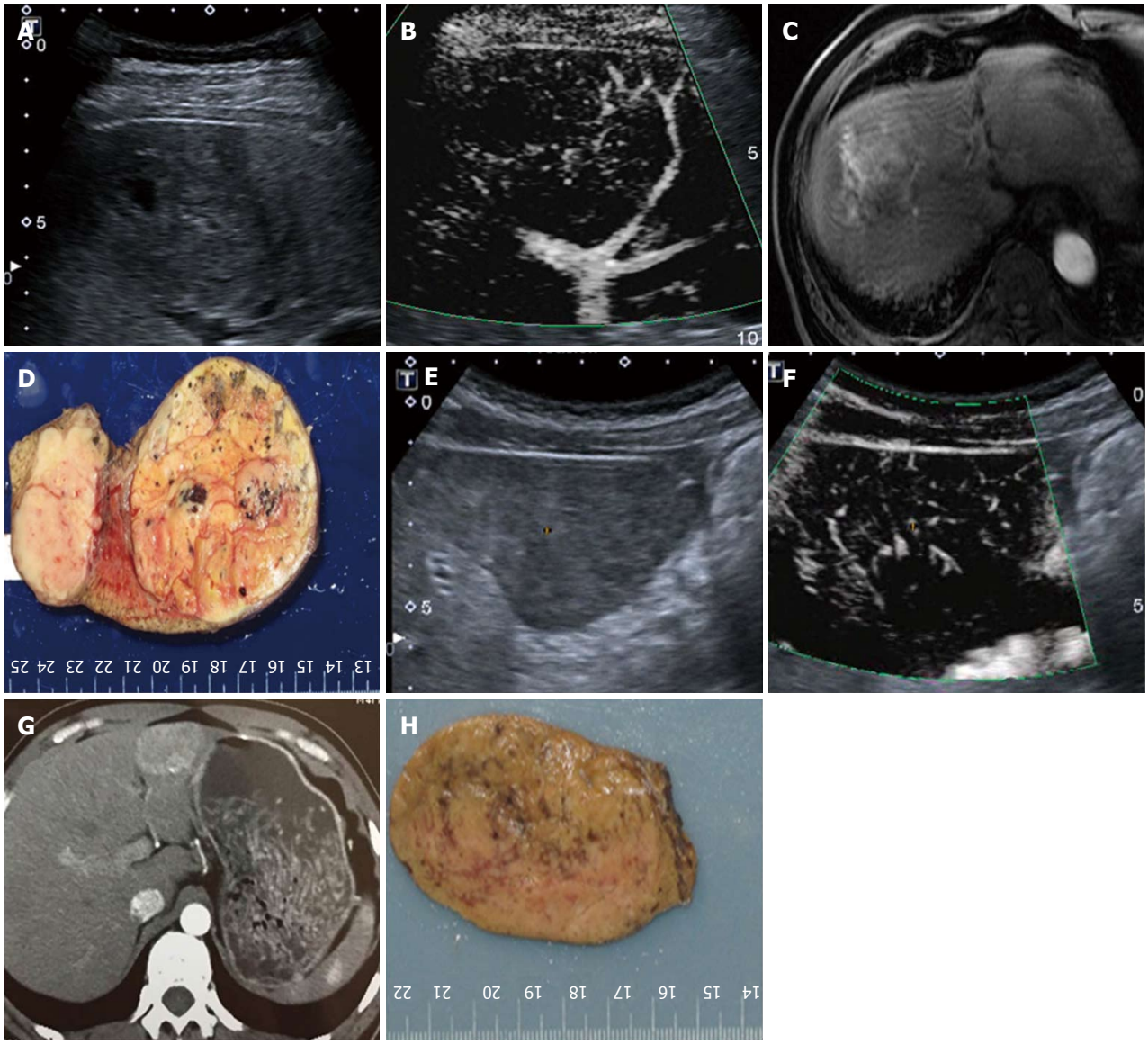

Figure 5 Diffuse honeycomb type (type Ⅳ). A-D: A 68-year-old male diagnosed with hepatic cellular carcinoma. A: A mixed-echo lesion with a relatively unclear margin was evident in the right liver lobe; B: SMI showed a diffuse honeycomb-distributed microvascular structure; C: Contrast-enhanced MRI showed diffuse enhancement of the lesion in the arterial phase; D: The pathology result showed that the inter-tumor blood vessels were distributed in a grid pattern resembling honeycombs. E-H: A 41-year-old male diagnosed with hepatic adenoma. E: A hypo-echo lesion with a clear margin was evident in the left liver lobe; F: SMI showed a diffuse honeycomb-distributed microvascular structure; G: Contrast-enhanced CT showed diffuse enhancement of the lesion in the arterial phase; H: The pathology result showed that the inter-tumor blood vessels were distributed in a grid pattern resembling honeycombs. SMI: Superb microvascular imaging.

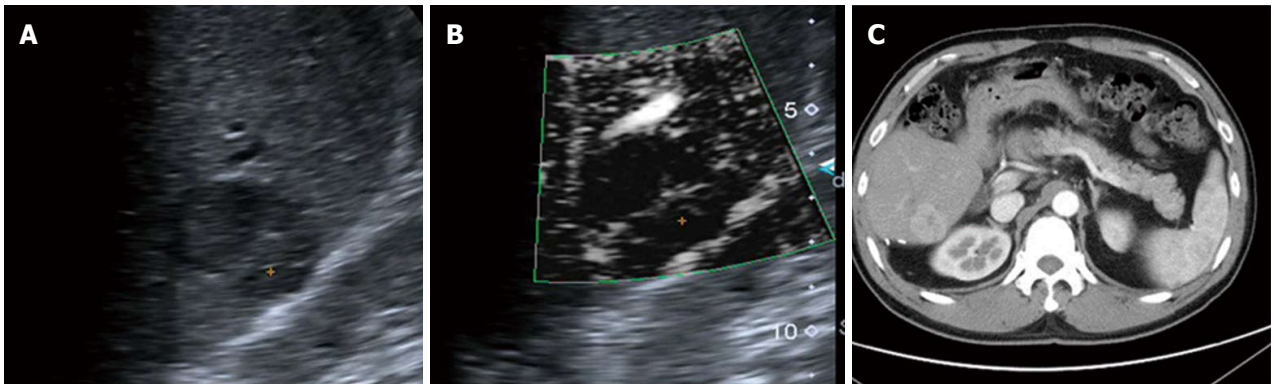

Figure 6 Non-specific type (type Ⅴ) in a 48-year old male diagnosed with hepatic cellular carcinoma. A: A low-echo lesion with a relatively clear margin was evident in the right liver lobe; B: SMI showed a microvascular distribution of a strip trunk with tiny branches ; C: Contrast-enhanced CT showed diffuse enhancement of the lesion in the arterial phase. SMI: Superb microvascular imaging.

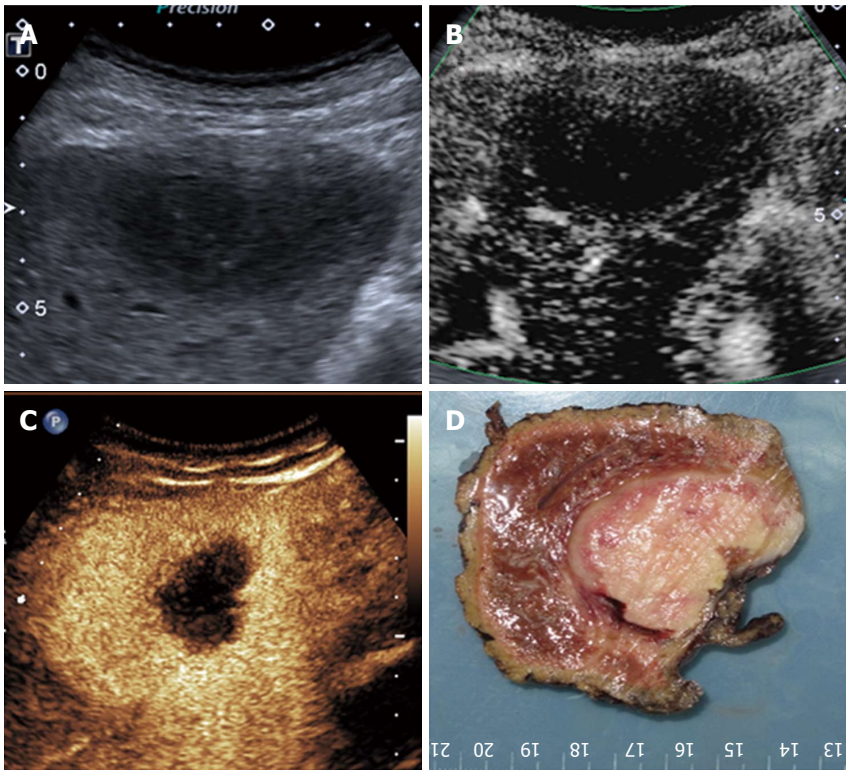

Figure 7 Thick rim type (type Ⅵ) in a 71-year-old male diagnosed with primary hepatic lymphoma. A: A low-echo lesion with a relatively clear margin was evident in the left liver lobe; B: SMI showed a thick rim-distributed microvascular structure; C: Contrast-enhanced ultrasound showed thick rim enhancement of the lesion in the arterial phase; D: The gross pathology result showed a thick rim distribution of the vasculature. SMI: Superb microvascular imaging.

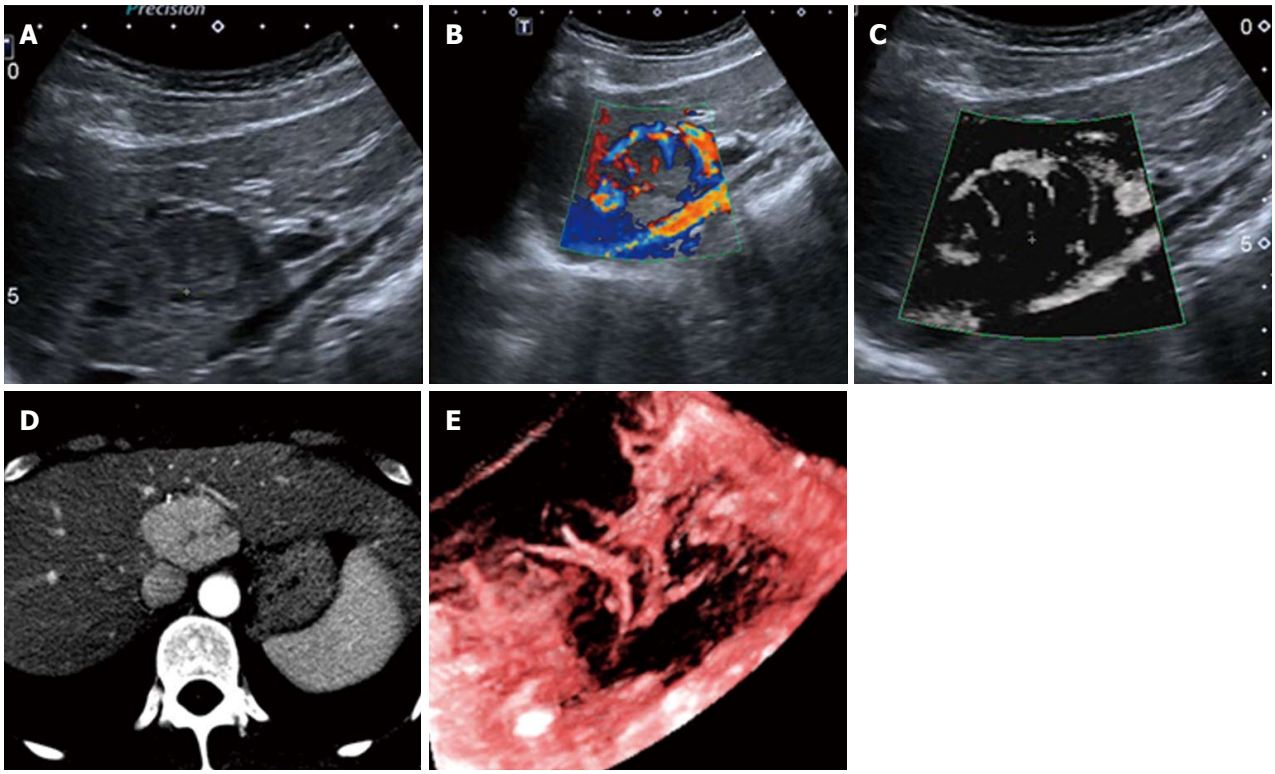

Figure 8 Spoke-wheel type (type Ⅶ) in a 39-year-old female diagnosed with focal nodular hyperplasia. A: A low-echo lesion with a relatively clear margin was evident in the caudate liver lobe; B: CDFI showed a spoke-wheel blood flow signal of this lesion; C: SMI showed a spoke-wheel-distributed microvascular structure; D: Contrast-enhanced CT showed diffuse enhancement with a central scar of the lesion in the arterial phase; E: 3-D vascular remodeling of this lesion was successfully achieved and showed spoke-wheel blood flow. SMI: Superb microvascular imaging.

may provide some helpful information for the diagnosis of some PHLs.

Our study has some limitations. First, for hepatic adenoma and primary hepatic lymphoma, the incidence rates are very low and sample errors are inevitable. Second, only nine lesions were pathologically diagnosed in this study. Therefore, a very low possibility of missed diagnosis remains for the other 22 lesions that were radiologically confirmed because as the results showed, different types of FLLs may have similar imaging manifestations despite the use of at least two kinds of enhanced imaging techniques.

In conclusion, SMI technology allows evaluation of the microvascular structures of FLLs without using any contrast agent. For HEs, the lesion size may affect SMI performance. SMI can overcome the limitation of CDFI, especially for micro-vessel descriptions in small lesions. The SMI characteristics between the most common malignant FLLs (HCCs and metastatic lesions) and the most common benign FLLs (HEs) are significantly different.

ARTICLE HIGHLIGHTS

Research background

The frequency of focal liver lesion (FLL) detection is increasing because of the development and prevalence of imaging technology, especially ultrasound examinations. The subsequent challenge not only involves efficiently distinguishing between malignant and benign FLLs but also precisely identifying the characteristics of all types of FLLs as different clinical treatments and outcomes may be inherent to each type.

Addressing this challenge involves choosing a diagnostic method that requires minimal time and effort, but can achieve high diagnostic accuracy. Some patients may be ineligible for the currently used imaging techniques, such as CEUS/CT/MRI, because of the risk of triggering or worsening renal failure due to contrast agents, such as iodine used for CT and Gd-DTPA (gadolinium diethylene-trianmine pentaacetic acid) used for MRI. In addition, the agents used in CEUS, CECT, and CEMRI are foreign bodies, and each one could cause hypersensitivity reactions. Additionally, the three techniques are expensive and time-consuming, limiting their widespread application.

Research motivation

Superb microvascular imaging (SMI) is a novel Doppler technique that simulates enhanced ultrasound by using advanced clutter elimination to obtain only vascular flow signals without using any contrast agent. The purpose of our study was to investigate the SMI features of focal liver lesions and to analyze their ability to provide additional information for differential diagnoses.

Research objectives

To explore the ability of SMI to differentially diagnose focal liver lesions and compare SMI morphologies to those of color Doppler ultrasound and enhanced imaging.

Research methods

Twenty-four patients with 31 focal liver lesions (FLLs) were included in our study, with diagnoses of hemangioma (HE) (n = 17), hepatocellular carcinoma (HCC) (n = 5), metastatic lesions (n = 5), primary hepatic lymphoma (n = 1), focal nodular hyperplasia (FNH) (n = 2), and adenoma (n = 1). Nine lesions were pathologically diagnosed, and 22 lesions were radiologically confirmed, all of which were evaluated by at least two types of enhanced imaging techniques. All patients had undergone SMI. Patients were divided into subgroups based on pathological and radiological diagnoses to analyze SMI manifestations. We also compared the SMI manifestations of the most common malignant FLLs of HCCs and metastatic lesions with those of the most common benign FLLs of HEs.

Research results

HEs were classified into three SMI subgroups: diffuse dot-like type (n = 6); strip rim type (n = 8); and nodular rim type (n = 3). The sizes of the three types of HEs were significantly different (P = 0.00, < 0.05). HCCs were classified into two subgroups: diffuse honeycomb type (n = 2) and non-specific type (n = 3). Four of the metastatic lesions were the strip rim type of HE, and the other metastatic lesion was the thick rim type, which is the same as that of lymphoma. FNH was described as a spoke-wheel type, and adenoma as a diffuse honeycomb type. The SMI types of HCCs and metastatic lesions were significantly different from that of HEs (P = 0.048, < 0.05).

Research conclusions

SMI technology enables microvascular evaluation of focal liver lesions without using any contrast agent. For HEs, lesion size may affect SMI performance. SMI is able to provide useful information for differentially diagnose HCCs and metastatic lesions from HEs.

REFERENCES

1 **Kaltenbach TE**, Engler P, Kratzer W, Oeztuerk S, Seufferlein T, Haenle MM, Graeter T. Prevalence of benign focal liver lesions: ultrasound investigation of 45,319 hospital patients. *Abdom Radiol* (NY) 2016; **41**: 25-32 [PMID: 26830608 DOI: 10.1007/s00261-015-0605-7]

2 **Mazzanti R**, Arena U, Tassi R. Hepatocellular carcinoma: Where are we? *World J Exp Med* 2016; **6**: 21-36 [PMID: 26929917 DOI: 10.5493/wjem.v6.i1.21]

3 **Chow PK**, Choo SP, Ng DC, Lo RH, Wang ML, Toh HC, Tai DW, Goh BK, Wong JS, Tay KH, Goh AS, Yan SX, Loke KS, Thang SP, Gogna A, Too CW, Irani FG, Leong S, Lim KH, Thng CH. National Cancer Centre Singapore Consensus Guidelines for Hepatocellular Carcinoma. *Liver Cancer* 2016; **5**: 97-106 [PMID: 27386428 DOI: 10.1159/000367759]

4 **Dietrich CF**, Sharma M, Gibson RN, Schreiber-Dietrich D, Jenssen C. Fortuitously discovered liver lesions. *World J Gastroenterol* 2013; **19**: 3173-3188 [PMID: 23745019 DOI: 10.3748/wjg.v19.i21.3173]

5 **Collin P**, Rinta-Kiikka I, Räty S, Laukkarinen J, Sand J. Diagnostic workup of liver lesions: too long time with too many examinations. *Scand J Gastroenterol* 2015; **50**: 355-359 [PMID: 25578122 DOI: 10.3109/00365521.2014.999349]

6 **Dietrich CF**, Maddalena ME, Cui XW, Schreiber-Dietrich D, Ignee A. Liver tumor characterization--review of the literature. *Ultraschall Med* 2012; **33** Suppl 1: S3-10 [PMID: 22723026 DOI: 10.1055/s-0032-1312897]

7 **Dietrich CF**. Liver tumor characterization--comments and illustrations regarding guidelines. *Ultraschall Med* 2012; **33** Suppl 1: S22-S30 [PMID: 22723025 DOI: 10.1055/s-0032-1312892]

8 **Hanahan D**, Weinberg RA. Hallmarks of cancer: the next generation. *Cell* 2011; **144**: 646-674 [PMID: 21376230 DOI: 10.1016/j.cell.2011.02.013]

9 **Bedoya M A,** White A M, Edgar J C, Pradhan M, Raab EL, MPH1, Meyer J S. Effect of Intravenous Administration of Contrast Media on Serum Creatinine Levels in Neonates. *Radiology* 2017; **284**: 160895 [DOI: 10.1148/radiol.2017160895]

10 **Kolenda C**, Dubost R, Hacard F, Mullet C, Le Quang D, Garnier L, Bienvenu J, Piriou V, Bérard F, Bienvenu F, Viel S. Evaluation of basophil activation test in the management of immediate hypersensitivity reactions to gadolinium-based contrast agents: a five-year experience. *J Allergy Clin Immunol Pract* 2017; **5**: 846-849 [PMID: 28341169 DOI: 10.1016/j.jaip.2017.01.020]

11 **Park AY**, Seo BK, Cha SH, Yeom SK, Lee SW, Chung HH. An Innovative Ultrasound Technique for Evaluation of Tumor Vascularity in Breast Cancers: Superb Micro-Vascular Imaging. *J Breast Cancer* 2016; **19**: 210-213 [PMID: 27382399 DOI: 10.4048/jbc.2016.19.2.210]

12 **Ma Y**, Li G, Li J, Ren WD. The Diagnostic Value of Superb Microvascular Imaging (SMI) in Detecting Blood Flow Signals of Breast Lesions: A Preliminary Study Comparing SMI to Color Doppler Flow Imaging. *Medicine (Baltimore)* 2015; **94**: e1502 [PMID: 26356718 DOI: 10.1097/MD.0000000000001502]
13 **Machado P**, Segal S, Lyshchik A, Forsberg F. A Novel Microvascular Flow Technique: Initial Results in Thyroids. *Ultrasound Q* 2016; **32**: 67-74 [PMID: 25900162 DOI: 10.1097/RUQ.0000000000000156]
14 **Zhan J**, Diao XH, Jin JM, Chen L, Chen Y. Superb Microvascular Imaging-A new vascular detecting ultrasonographic technique for avascular breast masses: A preliminary study. *Eur J Radiol* 2016; **85**: 915-921 [PMID: 27130051 DOI: 10.1016/j.ejrad.2015.12.011]
15 **Lee DH**, Lee JY, Han JK. Superb microvascular imaging technology for ultrasound examinations: Initial experiences for hepatic tumors. *Eur J Radiol* 2016; **85**: 2090-2095 [PMID: 27776663 DOI: 10.1016/j.ejrad.2016.09.026]
16 **Cong WM**, Bu H, Chen J, Dong H, Zhu YY, Feng LH, Chen J, Committee G. Practice guidelines for the pathological diagnosis of primary liver cancer: 2015 update. *World J Gastroenterol* 2016; **22**: 9279-9287 [PMID: 27895416 DOI: 10.3748/wjg.v22.i42.9279]
17 **Drudi FM**, Cantisani V, Gnecchi M, Malpassini F, Di Leo N, de Felice C. Contrast-enhanced ultrasound examination of the breast: a literature review. *Ultraschall Med* 2012; **33**: E1-E7 [PMID: 22623129 DOI: 10.1055/s-0031-1299408]
18 **Wu L**, Yen HH, Soon MS. Spoke-wheel sign of focal nodular hyperplasia revealed by superb micro-vascular ultrasound imaging. *QJM* 2015; **108**: 669-670 [PMID: 25614615 DOI: 10.1093/qjmed/hcv016]
19 **Massironi S,** Branchi F, Rossi R E, Fraquelli M, Elli L, Bardella MT, Cavalcoli F, Conte D. Hepatic hemangioma in celiac patients: data from a large consecutive series. *Gastroenterol Res Pract* 2015; **2015**: 749235
20 **Ishak K G,** Rabin L. Benign tumors of the liver. *Med Clin North Am* 1975; **59**: 995-1013 [DOI: 10.1016/S0025-7125(16)31998-8]
21 **Dong Y,** Zhu Z, Wang W P, Mao F, Ji ZB. Ultrasound features of hepatocellular adenoma and the additional value of contrast-enhanced ultrasound. *Hepatobiliary Pancreat Dis Int*, 2016; **15**: 48-54 [DOI: 10.1016/S1499-3872(15)60039-X]
22 **Padhan RK**, Das P, Shalimar. Primary hepatic lymphoma. *Trop Gastroenterol* 2015; **36**: 14-20 [PMID: 26591949 DOI: 10.7869/tg.239]
23 **Lu Q,** Zhang H, Wang W P, Jin YJ, Ji ZB. Primary non-Hodgkin's lymphoma of the liver: sonographic and CT findings. *Hepatobiliary Pancreat Dis Int* 2015; **14**: 75-81 [DOI: 10.1016/S1499-3872(14)60285-X]

P- Reviewer: Dietrich CF, Eleftheriadis NP, Tarantino G
S- Editor: Wei LJ **L- Editor**: Wang TQ **E- Editor**: Huang Y

Published by **Baishideng Publishing Group Inc**
7901 Stoneridge Drive, Suite 501, Pleasanton, CA 94588, USA
Telephone: +1-925-223-8242
Fax: +1-925-223-8243
E-mail: bpgoffice@wjgnet.com
Help Desk: http://www.f6publishing.com/helpdesk
http://www.wjgnet.com

ISSN 1007-9327